NUMERICAL PERFORMANCE ANALYSIS OF DELTA VORTEX GENERATOR LOCATED UPSTREAM OF IN-LINE TUBE BUNDLE

Mete ÖZŞEN [*]***, Sebiha YILDIZ***[1]

[*1]Department of Mechanical Engineering, Faculty of Mechanical Engineering, Yildiz Technical University, 34349, Istanbul, Turkey

[*] Corresponding author; E-mail: meteozsen@hotmail.com

The effect of the delta vortex generator located upstream of the in-line tube bundle on the heat transfer and pressure loss for cross-flow air was numerically investigated. The best accurate results were obtained by using the "Realizable k-epsilon" model with the "standard" wall function. In order to increase the accuracy of the numerical model, "production limit" and "curvature correction" coefficients that depend on the inlet air velocity were used. The average error in heat transfer and pressure loss in the range of Re=3000 and 13000 was obtained as 4.4% and 9.4%, respectively.

The distance between the tube bundle and vortex generator, angle of attack, and pitch were analyzed parametrically. In all vortex generator designs, upward secondary flows in front of tubes were observed between the rows. A maximum 16.6% improvement in the average Nusselt number and a maximum 42% penalty in pressure loss were obtained. The angle of attack is the parameter that affects the heat transfer the most. When the changes in both heat transfer and pressure loss are taken into account, for Re>9500, performance is positively affected with almost every vortex generator design.

Keywords*: Delta winglet, Vortex generator, In-line tube bundle, Numerical analysis, Heat transfer enhancement*

1. Introduction

Vortex Generators (VG) enhance heat transfer for finned or unfinned tubular heat exchangers using air as the external fluid. They increase mixing by creating secondary flows with vortices in the main flow [1]. The vortices improve heat transfer by reducing the boundary layer thickness [2]. In addition, VG reduces the wake region by directing the flow and provides better mixing of the flow [3].

Jacobi & Shah [1] reviewed studies investigating the physical mechanism of VG effects. In their study, it was stated that VG creates longitudinal vortices. Longitudinal vortices are vortex pairs rotating in the same or opposite direction and moving forward in the direction of the main flow. These longitudinal vortex pairs are called secondary flows in the main flow. Secondary flows occur near the surface and reduce the boundary layer thickness.

Zdanski *et al.* [4] placed delta winglets in front of an in-line tube bundle. It was found that there was a maximum increase of 30% in the average Nusselt number. The winglet pairs were placed in the first row of the finned tube heat exchanger in a "common flow up" layout by Kwak *et al.* [5] and Torii *et al.* [6]. Kwak *et al.* [5] obtained a 10-30% increase in heat transfer and a 34-55% reduction in pressure loss. Unlike the previous models [5, 6], delta winglets were added to all rows by Pal *et al.* [7]

and Arora *et al.* [8]. A maximum 64% [7] and %60 [8] improvement in heat transfer and a 58% [7] penalty in pressure loss were obtained. Agarwal & Sharma [9] used a different winglet shape, rectangular winglets, in the "common flow up" layout. The winglets were positioned one row apart, and the maximum increase in heat transfer was approximately 80%, with a corresponding pressure loss of about 38%. In addition, delta winglets in the "common flow down" layout were studied experimentally [10] and numerically [11, 12] on finned tube heat exchangers. VG were placed in all rows. The heat transfer saw a maximum improvement of 64% [10], 24% [11], and 60% [12] while the pressure loss experienced a penalty ranging from 20% to 44% [10]. Similarly, but this time with a rectangular winglet, Jang *et al.* [13] obtained a numerical 30% improvement in heat transfer and a 22% increase in pressure loss. A similar winglet shape, but this time for a tube bundle, was placed in the rear region of the tubes [14]. An increase of 10-50% in the Nusselt number was obtained. Another investigation on the placement of winglets in the rear region of the tube was studied by Abraham *et al.* [15]. The study focused on the taper winglet which is named as longitudinal winglet. An improvement in the Nusselt number between 12-38% and a reduction in the friction factor between 29-46% were observed. A splitter plate was used together with a delta winglet in finned tube heat exchangers by Jayavel & Tiwari [16]. With the splitter plate, it was aimed to reduce the extra pressure loss caused by the delta winglet, but it was stated that it had no effect.

Sarangi *et al.* [17] analyzed curved-trapezoidal shaped winglets, which did not have punched holes, as opposed to delta and rectangular winglets. Their analysis resulted in a 54.72% increase in heat transfer, albeit with an 8.4% deterioration in pressure loss. Another study investigating a different winglet shape, curved rectangular, was carried out by Gong *et al.* [18]. It is stated that an improvement in the Nusselt number between 15.4-21.6% and an increase of approximately 10% friction factor was obtained. Lin *et al.* [19] studied curved-trapezoidal shaped winglets with punched holes and obtained better thermal performance compared with curved rectangular shape studied by Gong *et al.* [18] for Re>1500. Another curved-shaped winglet called interrupted angular groove was investigated by Lin *et al.* [20]. Heat transfer augmentation was obtained, and the thermal performance factor under the same pumping power reached up to 1.2. Unlike the studies examining the single winglet shape, both delta and rectangular winglet forms were numerically analyzed simultaneously by Salviano *et al.* [21]. In addition, trapezoidal forms between these two forms were also analyzed simultaneously and an improvement in heat transfer ranging from 30% to 70% was obtained with deterioration in pressure loss between 20% and 90%.

Studies in the literature have shown that performance improvement is achieved by using VG in heat exchangers. These studies have also examined the parameters that dictate the position, layout, and design of the VG. Zdanski *et al.* [4] conducted an experimental investigation into the distance of the delta winglet to the tube bundle, the pitch value between the delta winglets, and the angle of attack. It was found that the angle value was the most influential parameter. Abraham *et al.* [15] investigated the length, base thickness, and tip thickness of the tapered winglet placed behind the tube. It was found that increasing the length improves the heat transfer but increases the pressure loss. The roll angle of rectangular winglets was investigated by Agarwal & Sharma [9]. It was emphasized that a winglet with a roll angle reduces the improvement provided by the winglet at the next row. Therefore, it was stated that only the winglets at the last row were given a roll angle. Sarangi *et al.* [17] numerically analyzed the radius of curvature, length of curvature, and the leading edge and rear end heights of the curved-trapezoidal winglet. It is observed that the curvature length is the most effective parameter on

the performance. Gong *et al.* [18] conducted another study where they analyzed the parameters of the curved winglet. Specifically, they examined the radius and length of the curvature, the height of the winglet, and the circumferential position of the winglet. Curvature radius and circumferential position were determined as the most effective parameters. Also, it is concluded with the same result by Sarangi *et al.* [17] that the winglet height does not affect the heat transfer. 20 different delta winglet positions and 4 different angles of attack were investigated by Arora *et al.* [22]. It was reported that the best position at angles smaller than 30° angle differed from the best position at larger angles. Among the studies in the literature, a wide range of parameters related to winglet position, angle, and shape have been analyzed by Salviano *et al.* [21]. It is found that designs closer to the rectangular winglet rather than the delta winglet give better thermal-hydraulic performance.

Lemouedda *et al.* [11] investigated two different winglet layouts at the same time. It is concluded that the "common flow up" layout is more suitable for staggered arrangement while the "common flow down" layout is more suitable for in-line arrangement. The experiment was replicated by Jang *et al.* [13], Torii *et al.* [6], and Valencia *et al.* [10], and the same results were achieved. In addition to the traditional layout ("common flow down" and "common flow up"), Wang [23] studied 2 new layouts called "front up rear down", and "front down rear up" and obtained better enhancement. Another comparison was made experimentally by Kwak *et al.* [5] on heat exchangers with different row numbers for the effect of winglets. It is observed that after the 3rd row, the effect of the winglet decreases. Salviano *et al.* [12] emphasized that instead of symmetrical layouts that are "common flow up" and "common flow down", an unsymmetrical layout has the best result.

The studies reviewed in the literature have tried to explain the effect of the VG by using air as the external fluid. In general, they concluded that the wake region behind the tube decreases and the mixing increases in this region.

In the studies available in the literature, generally "finned tube heat exchangers" are used to examine the effect of the winglet. On the other hand, there are few studies using tube bundles [4, 14, 15]. Among these studies, Mangrulkar *et al.* [14] and Abraham *et al.* [15] examined the effect of the winglet added behind the tube. The winglet used in their study was not used as VG. Apart from this, only Zdanski *et al.* [4] used the winglet as VG and performed an experimental study by placing it in the front region of the tube bundle.

The main objective of this study is to numerically investigate the effect of the VG placed in the front region of the tube bundle on the heat transfer, pressure drop, and thermal-hydraulic performance in the cross-flow of air over the tube bundle. In this study, the delta fin is placed in front of the tube bundle and the airflow through the tube bundle is numerically modeled. Zdanski et al, [4] did only experimental work on this subject; they developed a correlation from their experimental results. The numerical results of the present study are validated with the correlation of Zdanski *et al.* [4]. To explain the VG effect physically, flow and temperature distributions are obtained numerically. In addition, analyses were performed for 7 different designs with different values of the parameters which are the distance between delta winglet and tube bundle, winglet pitch, and angle of attack. The effects of the parameters on heat transfer, pressure drop, and thermal-hydraulic performance were analyzed. The parametric study aims to suggest a VG design that depends on the Re for practical use.

2. Numerical method

2.1. Computational domain

In this numerical study, tube bundle configuration studied experimentally by Zdanski *et al.* [4] was taken as a reference model (Fig. 1). Delta winglets are located in front of the tube bundle. VG is arranged side by side along the length of the tube with a pitch (*P*) value (Fig. 1.b). Dimensions are given in Tab. 1. To study different design parameters of VG, 11 different designs were given in Tab. 2 made by Zdanski *et al.* [4]. 7 of these designs are numerically modelled in this study.

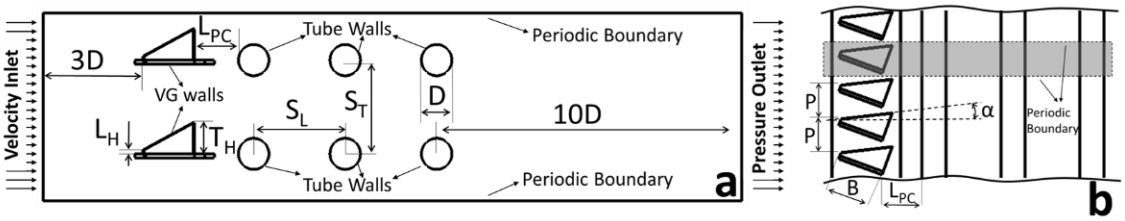

Figure 1. Computational domain a) Cross-section view b) Top view (Bounded area: Periodic domain)

Table 1. Tube bundle and VG dimensions [4]

Parameter	Dimension
S_T	46 mm
S_L	46 mm
D	16 mm
B	28 mm
T_H	16 mm
L_H	0 mm
L_{pc}	23.1mm – 31.1mm – 39.1 mm
α	20° - 30° - 40°
P	20.5mm – 26.4mm – 37mm

Table 2. VG parameter values [4]

Design	1	2	3	4	5	6	7	8	9	10	11
P [mm]	20.5	20.5	20.5	26.4	26.4	26.4	26.4	26.4	37.0	37.0	37.0
L_{pc}[mm]	23.1	31.1	39.1	23.1	31.1	31.1	31.1	39.1	23.1	31.1	39.1
α [°]	20	20	20	20	20	30	40	20	20	20	20

As shown in Fig.1a, the flow analysis was performed using the "velocity inlet" boundary condition for the inlet, the "pressure outlet" boundary condition for the outlet, and the "periodic boundary condition" for the side and top surfaces. In addition, the "constant heat flux" and "non-slip" conditions were applied to the tube surfaces, and the "non-slip" condition was also applied to the VG surfaces.

In the transverse direction, the tubes are placed periodically as ST value. The upper and lower surfaces were given periodic boundary conditions as stated in Fig. 1.a. The flow is similar at each cross-section along the tube length. A small section in this direction is modelled. A 3-dimensional model with a length equal to the pitch (P) value was created (the bounded region shown in Fig. 1.b).

The numerical model is extended by 3 times and 10 times the tube diameter at the air inlet and air outlet, respectively (Fig. 1.a). The purpose of the extension at the air inlet is to ensure velocity uniformity, while the purpose of the extension at the air outlet is to prevent the backward flow effect.

2.2. Numerical model

In the referenced experimental study, tubes were used as electric rod heaters. To accurately model the heat transfer from these heaters to the air, it was necessary to solve not only the continuity and momentum conservation equations but also the energy conservation equations. The study assumed a steady state, turbulent, three-dimensional, and incompressible flow with constant physical properties. Hence governing equations that are continuity, momentum, and energy conservation equations shown in Eq. (1), (2) and (3) respectively.

$$\frac{\partial}{\partial x_j}(\rho u_j) = 0 \tag{1}$$

$$\frac{\partial}{\partial x_j}(\rho u_i u_j) = -\frac{\partial p}{\partial x_i} + \frac{\partial}{\partial x_j}\left[\mu\left(\frac{\partial u_i}{\partial x_j} + \frac{\partial u_j}{\partial x_i}\right)\right] + \frac{\partial}{\partial x_j}\left(-\rho\overline{u_i' u_j'}\right) \tag{2}$$

$$\frac{\partial}{\partial x_j}(\rho u_j T) = \frac{\partial}{\partial x_j}\left(\frac{\mu}{Pr}\frac{\partial T}{\partial x_j} - \rho\overline{T' u_j'}\right) \tag{3}$$

$\rho\overline{u_i' u_j'}$ and $\rho\overline{T' u_j'}$ represent Reynolds stress and turbulent heat flux respectively.

To account for turbulence effects, "Realizable k-epsilon", "RNG k-epsilon" and "k-omega SST" turbulence models were used in the analyses. In the literature, studies on tube bundles and VG have obtained appropriate results with different turbulence models. Salviano *et al.* [21] and Sarangi *et al.* [17] with the "k-omega SST" model, Naik & Tiwari [24] with the "Realizable k-epsilon" model and Arora *et al.* [8] with the "RNG k-epsilon" model found appropriate results. To calculate the values near the wall more precisely, it is suggested to use various wall functions [25]. Among the suggested "Standard", "enhanced" and "scalable" wall functions were used. In addition, turbulence models are supported with various correction factors to increase their accuracy. "Production limit" and "curvature correction" factors were used in this study.

In the ideal case, electrical energy is directly converted into thermal energy; however, in practical scenarios, some of this thermal energy is inevitably lost to the surroundings, predominantly through radiation. The heat loss rate was determined to be 7% by Zdanski *et al.* [4]. Information about electrical heater power and dimensions was taken from Pauli [26]. The length of each electric heater is L = 0.17 m and its diameter is D = 0.016 m. In total, 6 electric heaters were used. When the heat transfer area of an electric heater surface is calculated as πDL, the total heat transfer surface area is 6 times as large. The total heat transfer surface area is approximately A_s= 0.05127 m^2. The total power of 6 electric heaters is 200 W. The total ideal heat flux obtained by dividing the total electric heater power by the heat transfer area is approximately 3900.856 W/m^2. When heat loss is taken into account as 7%, the heat flux from the electric heater surfaces to the air is calculated as q"=3628 W/m^2.

The air inlet temperature was assumed to be homogeneous and 25 °C. An experimental study was carried out between Re=3000 and Re=13000. To obtain Re values in this range, air inlet velocities were defined between 2.5 m/s and 9.5 m/s. The inlet velocity was assumed to be homogeneous. Atmospheric pressure condition was applied at the air outlet surface.

The numerical model was created and solved with "ANSYS Fluent 2021 R2". For pressure-velocity coupling, the SIMPLE algorithm was selected. The second order upwind scheme was used for

all discretization. Maximum residual obtained 10^{-6} for energy, momentum and turbulence equations and 10^{-4} for continuity equation. To ensure that the solution was converged, the area average temperature at the outlet and pressure at the inlet were checked during the iteration process. It was seen that these flow variables reached steady before completing iteration. This indicates that the solution is assumed to have converged.

2.3. Grid independence

Grid independence analysis for the tube bundle was performed with 6 different grid structures for Re=12250 (inlet velocity of 9 m/s). To obtain different grid structure while all mesh settings were fixed, only mesh growth rate value was set as 1.5, 1.25, 1.1, 1.025, and 1. In addition, to reach the maximum element number mesh element size was decreased from 0.0181mm to 0.0016mm after the mesh growth rate was decided to as 1.025. It is noted that all mesh structure has inflation layers on tube surfaces with 20 layers and 1.1 inflation growth rate. As can be seen from the Fig. 2, the variation in the average Nusselt number is very small in the last three meshes. To shorten the numerical calculation time, the third to last mesh structure was selected for further analyses.

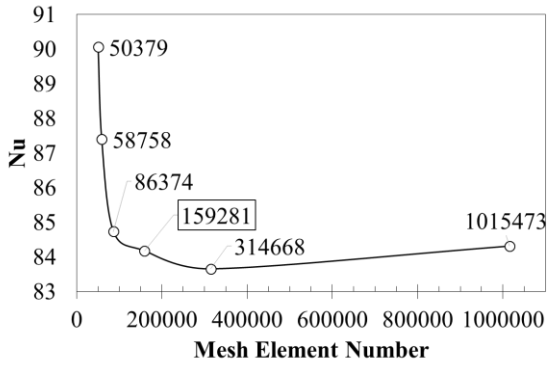

Figure 2. Grid independency analysis on Nusselt number for tube bundle at Re=12250

After determining the settings for the fine mesh structure, the fine boundary layer structure was obtained as shown in Fig. 3.a. For 9 m/s inlet velocity, the maximum value of y^+ on the tube surface was obtained as "1". As shown in Fig. 3.b, a fine mesh structure with 545162 elements was obtained.

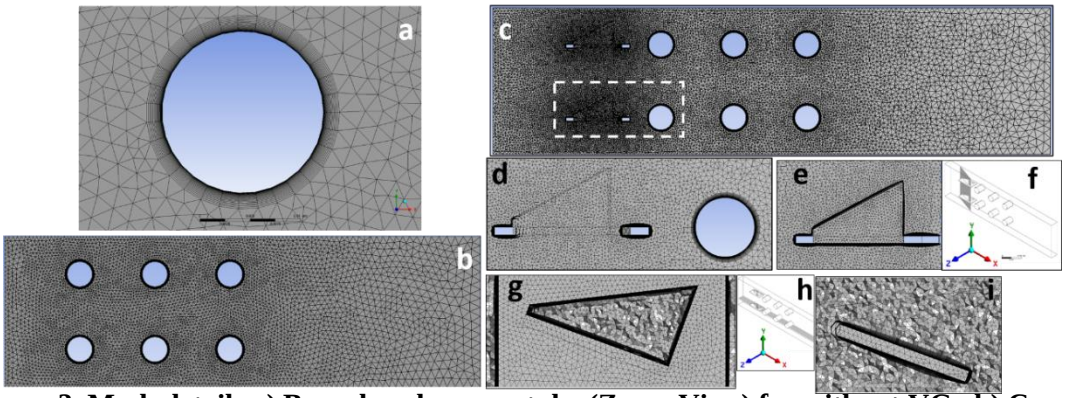

Figure 3. Mesh details a) Boundary layer on tube (Zoom View) for without VG, b) Cross-section view of tube bundle without VG, c) Cross-section view of tube bundle with VG, d) Section stated with dashed rectangular in Fig. 3.c, e) Near vortex generator on plane has alfa angle shown in Fig. 3.f, g) Near vortex generator base plane on ZX plane shown in Fig. 3.h, i) Near vortex generator at 4mm up from ZX plane shown in Fig. 3.h.

For the VG analyses, in addition to the grid adjustments obtained for the tube bundle, VG surface boundary layer improvement study was performed on "Design No 1" (see Tab. 2). For 9 m/s inlet velocity, the maximum value of y^+ on the VG surfaces is 1.4, while the average value is 0.56. The fine mesh has a number of 1760377 elements as shown in Fig. 3.c. The boundary layer details on the VG surfaces were given in Fig. 3.d-i in different views.

2.4. Validation

The physical properties of the air used in the calculations were taken at film temperature. The film temperature was calculated by averaging the tube surface temperature and the air inlet temperature. The tube surface temperature was obtained from the numerical results as the area-weighted average of the temperature on the tube surfaces. The same tube surface temperature value was also used in the calculation of the average heat convection coefficient as shown in Eq. (4). This average heat transfer coefficient was used for calculating the average Nusselt number as shown in Eq. (5).

$$\mathrm{h} = q"/(T_S - T_i) \tag{4}$$

$$\mathrm{Nu} = hD/k \tag{5}$$

Validation was made for the whole Re range. To obtain results in the Re range, analysis was repeated with different air inlet velocities that are 2, 3, 4, 5, 6, 8, 9, and 9.5 m/s. In addition, analyses were repeated to obtain results for each different turbulence model approximation. Fig. 4. shows the comparison between results of the analyses and Grimison's [27] correlation that is used by reference experimental study [4] and is calculated by Eq. (6). In addition, numerical results were also compared with Zhukauskas [28] correlation in Fig. (4). Air physical properties were taken at average temperature of inlet and outlet of the air for Zhukauskas [28] correlation shown in Eq. (7).

$$\mathrm{Nu}_{Grimison} = 0.24882\ Re^{0.608} \tag{6}$$

$$Nu_{Zhukauskas} = 0.2322\ Re^{0.63} Pr^{0.36}\ (Pr/Pr_s)^{0.25} \tag{7}$$

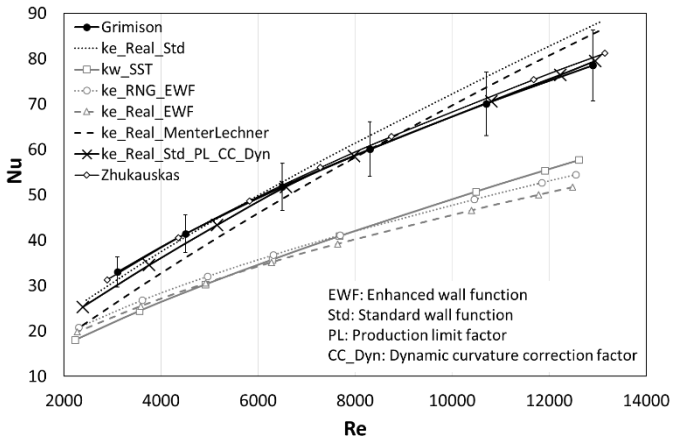

Figure 4. Different numerical approaches comparisons with Grimison [27] and Zhukauskas [28] correlation for average Nusselt number for tube bundle (Error bar states 10% range)

Validation analysis was made based on Grimison's [27] correlation. The "Realizable k-epsilon" turbulence model with the "standard" wall function is the closest among the numerical approximations. Turbulence model correction factors were added in addition to the use of the "realizable k-epsilon" turbulence model with the "standard" wall function. Initially, the 'Production Limit' factor was incorporated, which resulted in a slight improvement in convergence. Subsequently, the 'Curvature Correction Factor (CCF)' was introduced. This led to a significant enhancement in convergence for Re>9000 and effectively corrected the overestimation. However, it was observed that for Re<5000, the convergence deteriorated and exceeded the limit. This result showed that the effect of the curvature correction factor should be reduced as the Re decreases. To achieve this, the value of the curvature correction factor was changed depending on the air inlet velocity. This is called the dynamic curvature correction factor that is adjusted according to the rule shown in Eq. (8), (9) and (10). After adding correction factors, numerical results get much closer. The maximum difference is 6.83% and the absolute average difference is 1.84% between 3000 and 13000 Re which is the experimental range. Differences are in in 10% error bar range which means results are in good agreement with Grimison's empirical correlation for in-line tube bundle. In addition, numerical results are also in good agreement with Zhukauskas's [28] empirical correlation. The maximum difference is 8.1% while the average difference is 3.86%.

$$CCF=1.12 \qquad V>9.5\ m/s \tag{8}$$

$$CCF=0.2375\,V-1.1375 \qquad 5\leq V\leq 9.5\ m/s \tag{9}$$

$$CCF=0.05 \qquad V<5\ m/s \tag{10}$$

The average Nusselt number obtained by the VG numerical analyses was compared with the correlation obtained by Zdanski *et al.* [4] which calculated by Eq. (11) and (12). The turbulence model, wall function and correction factor approaches, which were found appropriate for the tube bundle analyses, were also used in the VG analyses. As a result, the maximum and absolute average differences are 13.3% and 4.4% respectively.

$$Nu_{Zdanski} = 0.26557\, Re^{0.608}\, C_L\, (P/D)^{-0.075}\, cos(\alpha)^{-0.448} \tag{11}$$

$$C_L = -0.1393\left(L_{pc}/D\right)^2 + 0.5525\left(L_{pc}/D\right) + 0.4758 \tag{12}$$

The approaches found suitable for heat transfer were evaluated in terms of pressure loss. The maximum difference between numerical and experimental pressure loss values is 22.7% while the absolute mean difference is 8.6%.

3. Results and discussion

The results for the case of Re=5200 (inlet velocity of 4 m/s) are used for temperature and flow distribution. The analysis results are presented in the cross-section view.

To explain the VG effect, the tube bundle result was compared with only "Design 7" in Fig. 5. For other VG designs the mechanism of the VG effects is the same. When comparing temperature distribution in Fig. 5. a and c, the regions between the tube rows in with VG designs are colder than the tube bundle without VG. This shows that the flow is better mixed in the designs with VG. In this way, the temperature difference between the air and front surfaces of the tubes in the 2nd and 3rd rows increased and heat transfer increased. The reason for this result can be clearly understood when the

streamlines in Fig. 5. d are examined. In VG design, it is seen that secondary flows occur upwards on the front of the tubes in the 2nd and 3rd rows. Thanks to these secondary flows, the main flow is directed to these regions and mixing is provided. In this way, the cooler air in the main flow contacts the hot tube surface and increases heat transfer. These secondary flows also mean that the wake region between the tubes is reduced. This is clearly seen in the 2nd cavities of the designs with VG.

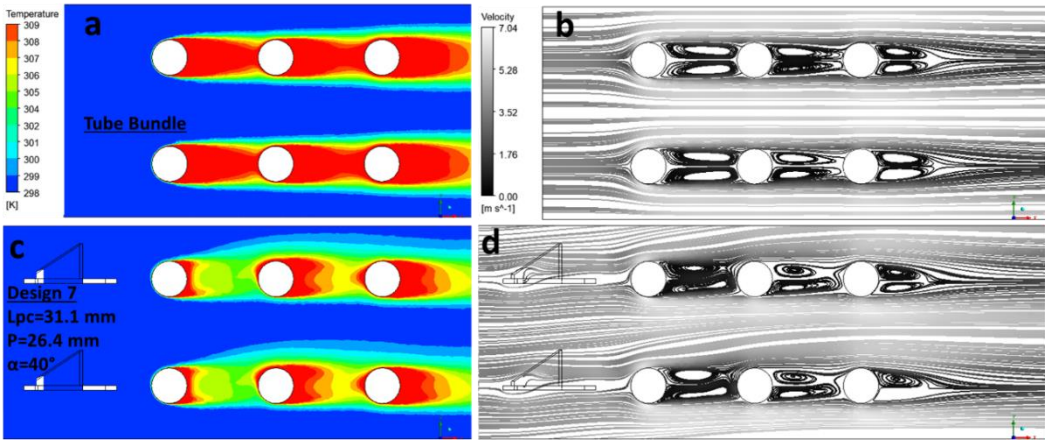

Figure 5. Temperature distributions (a, c) and streamlines (b, d) on XY plane at middle surface (Z-direction) at Re=5200 for tube bundle (a, b) and VG "design no 7" (c, d)

Temperature differences between designs are shown in Fig. 6. Designs shown in Fig. 6 are the designs that have the best value for each parameter according to temperature decrease. For example, "Design No 1" has the best L_{pc} value. It can be observed that in all VG designs, temperatures are less than the tube bundle. A maximum temperature decrease of 6.44 K in the 1st space and 3.46 K in the 2nd space was observed with VG. This indicates that the effect of the VG decreases in the flow direction in the next rows. In accordance with this result, Kwak *et al.* [5] also stated that the effect of the VG decreased after the 3rd row.

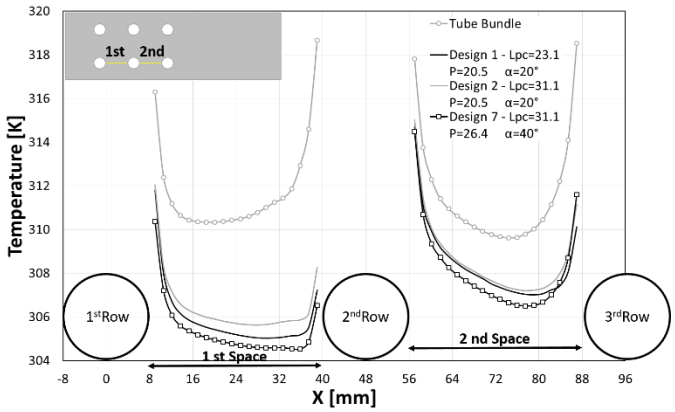

Figure 6. Temperature distribution through line between tube centers at bottom tubes for Re=5200

Another examination that proves the improvement of heat transfer can be done by analyzing the tube surface temperatures. Since a constant heat flux is given to the tube surfaces, the best heat transfer is obtained when the tube surface temperature is the lowest. When the average tube surface temperatures are examined, 343.68 K temperature is obtained in the tube bundle without VG, while 340.1, 340.3, 340.6, 340.5, 339.5, 338.4, and 341.3 K temperatures are obtained in "Design No 1, 2, 3,

5, 6, 7 and10" respectively. It is concluded that temperatures in all VG designs are smaller than the tube bundle. That means that heat transfer is improved for all VG designs. At α=40° ("Design No 7"), a temperature decrease of 5.25 K was obtained and it is the highest temperature drop among all the designs.

For examining the effects of parameters in the whole Re range, the value of the percentage improvement of the Nusselt number was calculated and shown in Fig. 7.a. To investigate the effects of the distance (L_{pc}) parameter, the results of "Design No 1, 2 and 3" are compared. According to the results for Re>5000, when the distance between the VG and the tube bundle increases from L_{pc} =23.1mm to L_{pc} =31.1mm, the heat transfer improves and when the distance increases further, the heat transfer worsens when L_{pc}=39.1mm. This shows that L_{pc} has an optimum value when evaluated in terms of heat transfer. A Similar result was obtained experimentally by Zdanski *et al.* [4]. The heat transfer improvement decreased as pitch (P) increased according to "Design No 2, 5 and 10" while improvement increased as the angle (α) increased according to "Design No 5, 6 and 7". For all Re ranges, the highest improvement was obtained at α=40°. This means that the angle parameter is the parameter that affects the heat transfer more.

While VG improves heat transfer, it increases pressure loss. The percentages of increase with respect to the tube bundle without VG are given in Fig. 7.b. At approximately Re<7000 pressure loss increase rate is not changed with changing L_{pc}. For P and α parameters, effects on pressure loss are the same as the effect on heat transfer for all Re ranges. Both heat transfer and pressure loss increase with an increasing α while they decrease with a decrease in P. In addition, it can be clearly seen that the most increment occurred at "Design No 7" (α=40°). This design is the best in view of heat transfer although the worst design in view of pressure loss.

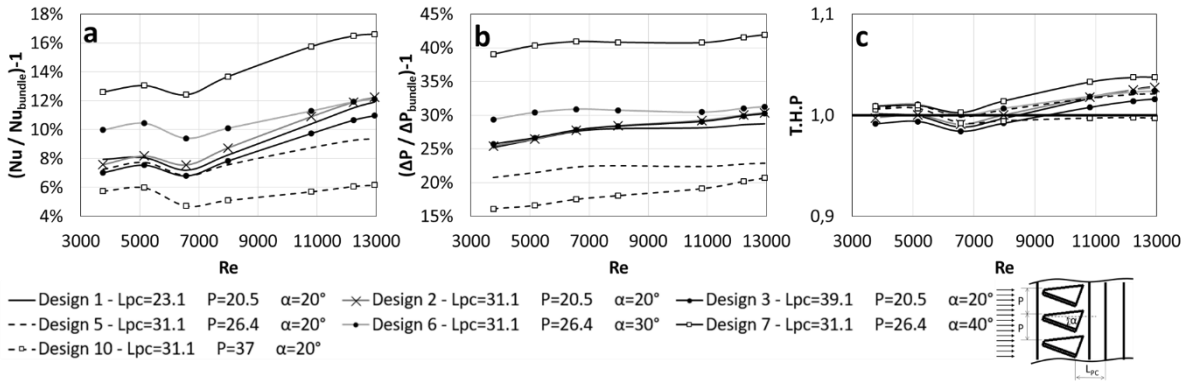

Figure 7. Effect of the VG a) Nusselt number improvement percentage b) Pressure drop increment percentage c) Thermal-Hydraulic Performance

To determine the best performance among the designs, both the improvement in heat transfer and deterioration in pressure loss should be considered. Therefore, the "thermal-hydraulic performance" (T.H.P) parameter should be calculated as shown in Eq. (13). T.H.P values of all designs are shown in Fig. 7.c. Performance values are very close to the minimum limit of 1. Performance values between designs are also close to each other. Improvement in heat transfer was obtained in all designs with VG. However, considering the increase in pressure loss, it should be noted that there is a performance improvement in designs where the thermal-hydraulic performance value is above "1". When Fig. 7.c is analyzed, the T.H.P value is above 1 for almost every VG design when Re

is greater than 9500, while it varies at lower Re. The performance of "Design No 7" with the largest angle α=40° is above 1 in all Re ranges. Therefore, it can be considered as the best design.

$$T.H.P = (Nu \,/\, Nu_{bundle}\,)/(\Delta P \,/\, \Delta P_{bundle}\,)^{(1/3)}) \tag{13}$$

4. Conclusions

The physical mechanism of the effect of the VG located in front of the tube bundle on the thermal and hydraulic performance was investigated numerically. Average errors of 4.4% and 9.4% were obtained in terms of heat transfer and pressure loss respectively. The effect of the design parameters of VG was also investigated. The distance between the VG and tube bundle (L_{pc}), pitch (P) and angle of attack (α) parameters were analyzed. In general, the following results were obtained:

- In the designs with VG, it was observed that there are upward air flows on the front surfaces of the tubes in the 2nd and 3rd rows. Thanks to these secondary flows, the main flow is directed to the region between rows and increases the mixture. This is the main mechanism of the VG that increases heat transfer.
- The upward secondary flows observed between the rows reduced the wake region. The reduction of the wake region also has a positive effect on heat transfer.
- In designs with VG, the air temperature of the region between the rows is lower than the tube bundle without VG. Also, the average tube surface temperatures are lower in designs with VG.
- VG angle of attack (α) is the parameter that affects the heat transfer the most. The Nusselt improvement value increased the most as the angle value increased. The highest improvement value of 16.6% was obtained with the highest angle of 40°. In addition, the highest pressure loss deterioration value of 42% was also obtained at the highest angle value of 40°.
- Heat transfer and pressure loss increases with decreasing pitch.
- The distance of the VG to the tube bundle has an optimum point. Maximum heat transfer improvement is achieved at a certain distance. As it moves away from or closer to this value, the heat transfer improvement decreases.
- While "Design No 7" (L_{pc} =31.1mm, P=26.4mm and α=40°) is the best design for all Re in terms of heat transfer, it is the best design for approximately Re>6000 in terms of T.H.P. While Re<6000 “Design No 6” is slightly better than “Design No 7”, it can be suggested that “Design No 7” can be applied for any Re.
- For Re>9500, it can be assumed that performance improvement will occur with almost any VG design. For lower Re, care should be taken in the selection of design parameters.
- One of the most important results is that the surface temperature decreases when using VG. In practice, this means that for any air handling unit system, the same electric heaters can be used with more power without reaching high surface temperatures.
- To increase T.H.P, parametric studies should be made with many more parameters for example winglet length (B), winglet front (L_H) and rear height (T_H), shape of winglet, etc. Further investigations are needed to optimize the use of VG in the in-line tube bundle.

Acknowledgment

The authors would like to acknowledge that this paper is submitted in partial fulfillment of the requirements for the Ph.D. degree at Yildiz Technical University.

Nomenclature

A_s	Heat transfer surface area [m^2]
B	vortex generator length [m]
CCF	curvature correction factor [-]
C_L	geometric coefficient of Zdanski average Nu correlation [-]
D	tube diameter [m]
h	average heat transfer coefficient [$Wm^{-2}K^{-1}$]
k	air thermal conductivity [$Wm^{-1}K^{-1}$]
L_H	front height of delta vortex generator [m]
L_{pc}	distance between vortex generator and tube bundle [m]
Nu	average Nusselt number [-]
Nu_{bundle}	average Nusselt number of tube bundle [-]
P	pitch [m]
Pr	Prandtl number
Pr_s	Prandtl number at surface temperature [-]
p	pressure [Pa]
q"	heat flux [Wm^{-2}]
Re	Reynolds number ($= \rho\ V_{max}\ \ D/\mu$), [-]
S_L	longitudinal pitch between tubes [m]
S_T	transverse pitch between tubes [m]
T	temperature [K]
T_H	rear height of delta vortex generator [m]
T_i	air inlet temperature [K]
T_S	tube surface temperature [K]
T.H.P	thermal hydraulic performance [-]
u_i, u_j	velocity component [m/s]
VG	vortex generators
V	air inlet velocity – free stream velocity [m/s]
V_{max}	maximum air velocity occurring within the tube bundle ($S_T\ V/(S_T - D)$) [m/s]
Greek Symbols	
α	angle of attack of vortex generator [rad]
ρ	density of air [kgm^{-3}]
μ	dynamic viscosity of the air [Nsm^{-2}]
ΔP_{bundle}	pressure drop of tube bundle [Pa]

References

[1] Jacobi, A. M., Shah, R. K., Heat Transfer Surface Enhancement Through The Use Of Longitudinal Vortices: A Review Of Recent Progress, *Experimental Thermal and Fluid Science, 11* (1995), 3, pp. 295-309

[2] Kataoka, K., *et al.*, Heat/Mass Transfer In Taylor Vortex Flow With Constant Axial Flow Rates, *International Journal of Heat and Mass Transfer, 20* (1977), 1, pp. 57-63

[3] Sadeghianjahromi, A., Wang, C.-C., Heat Transfer Enhancement In Fin-And-Tube Heat Exchangers – A Review On Different Mechanisms, *Renewable and Sustainable Energy Reviews, 137* (2021), pp. 110470 https://doi.org/10.1016/j.rser.2020.110470

[4] Zdanski, P. S. B., *et al.*, Effects Of Delta Winglet Vortex Generators On Flow Of Air Over In-Line Tube Bank: A New Empirical Correlation For Heat Transfer Prediction, *International Communications in Heat and Mass Transfer, 67* (2015), pp. 89-96 http://dx.doi.org/10.1016/j.icheatmasstransfer.2015.07.010

[5] Kwak, K. M., *et al.*, Heat Transfer And Pressure Loss Penalty For The Number Of Tube Rows Of Staggered Finned-Tube Bundles With A Single Transverse Row Of Winglets, *International Journal of Heat and Mass Transfer, 46* (2003), 1, pp. 175-180

[6] Torii, K., *et al.*, Heat Transfer Enhancement Accompanying Pressure-Loss Reduction With Winglet-Type Vortex Generators For Fin-Tube Heat Exchangers, *International Journal of Heat and Mass Transfer, 45* (2002), 18, pp. 3795-3801

[7] Pal, A., *et al.*, Enhancement Of Heat Transfer Using Delta-Winglet Type Vortex Generators With A Common-Flow-Up Arrangement, *Numerical Heat Transfer, Part A: Applications: An International Journal of Computation and Methodology, 61* (2012), 12, pp. 912-928

[8] Arora, A., *et al.*, Numerical Optimization Of Location Of 'Common Flow Up' Delta Winglets For Inline Aligned Finned Tube Heat Exchanger, *Applied Thermal Engineering, 82* (2015), pp. 329-340 http://dx.doi.org/10.1016/j.applthermaleng.2015.02.071

[9] Agarwal, S., Sharma, R. P., Numerical Investigation of Heat Transfer Enhancement Using Hybrid Vortex Generator Arrays in Fin-and-Tube Heat Exchangers, *Journal of Thermal Science and Engineering Applications, 8* (2016), 3, pp. 031007 1-9

[10] Valencia, A., *et al*. Heat Transfer And Flow Loss In A Fin-Tube Heat Exchanger Element With Wing-Type Vortex Generators, *Institution of Chemical Engineers Symposium Series, 1* (1992), pp. 327-333

[11] Lemouedda, A., *et al.*, Optimization Of The Angle Of Attack Of Delta-Winglet Vortex Generators In A Plate-Fin-And-Tube Heat Exchanger, *International Journal of Heat and Mass Transfer, 53* (2010), 23-24, pp. 5386-5399

[12] Salviano, L. O., *et al.*, Optimization Of Winglet-Type Vortex Generator Positions And Angles In Plate-Fin Compact Heat Exchanger: Response Surface Methodology And Direct Optimization, *International Journal of Heat and Mass Transfer, 82* (2015), pp. 373-387 http://dx.doi.org/10.1016/j.ijheatmasstransfer.2014.10.072

[13] Jang, J.-Y., *et al.*, Optimization Of The Span Angle And Location Of Vortex Generators In A Plate-Fin And Tube Heat Exchanger, *International Journal of Heat and Mass Transfer, 67* (2013), pp. 432-444 http://dx.doi.org/10.1016/j.ijheatmasstransfer.2013.08.028

[14] Mangrulkar, C. K., *et al.*, Experimental And CFD Prediction Of Heat Transfer And Friction Factor Characteristics In Cross Flow Tube Bank With Integral Splitter Plate, *International Journal of Heat and Mass Transfer, 104* (2017), pp. 964-978 http://dx.doi.org/10.1016/j.ijheatmasstransfer.2016.09.013

[15] Abraham, J. D., *et al.*, Numerical Analysis For Thermo-Hydraulic Performance Of Staggered Cross Flow Tube Bank With Longitudinal Tapered Fins, *International Communications in Heat and Mass Transfer, 118* (2020), pp. 104905 https://doi.org/10.1016/j.icheatmasstransfer.2020.104905

[16] Jayavel, S., Tiwari, S., Effect of Vortex Generators and Integral Splitter Plate on Heat Transfer and Pressure Drop for Laminar Flow Past Channel-Confined Tube Banks, *Heat Transfer Engineering, 31* (2010), *5*, pp. 383-394

[17] Sarangi, S. K., *et al.*, Analysis And Optimization Of The Curved Trapezoidal Winglet Geometry In A Compact Heat Exchanger, *Applied Thermal Engineering, 182* (2021), pp. 116088 https://doi.org/10.1016/j.applthermaleng.2020.116088

[18] Gong, B., *et al.*, Heat Transfer Characteristics Of A Circular Tube Bank Fin Heat Exchanger With Fins Punched Curve Rectangular Vortex Generators In The Wake Regions Of The Tubes,

Applied Thermal Engineering, 75 (2015), pp. 224-238
http://dx.doi.org/10.1016/j.applthermaleng.2014.09.043

[19] Lin, Z., et al., Heat Transfer Augmentation Characteristics Of A Fin Punched With Curve Trapezoidal Vortex Generators At The Rear Of Tubes, *Thermal Science, 26* (2022), *4B*, pp. 3529-3544

[20] Lin, Z., et al., Parametric Effect Of The Interrupted Annular Groove Fin On Flow And Heat Transfer Characteristics Of A Finned Circular Tube Heat Exchanger, *Thermal Science, 26* (2022), *6A*, pp. 4503-4517

[21] Salviano, L. O., *et al.*, Thermal-Hydraulic Performance Optimization Of Inline And Staggered Fin-Tube Compact Heat Exchangers Applying Longitudinal Vortex Generators, *Applied Thermal Engineering, 95* (2016), pp. 311-329 http://dx.doi.org/10.1016/j.applthermaleng.2015.11.069

[22] Arora, A., *et al.*, Development Of Parametric Space For The Vortex Generator Location For Improving Thermal Compactness Of An Existing Inline Fin And Tube Heat Exchanger, *Applied Thermal Engineering, 98* (2016), pp. 727-742 http://dx.doi.org/10.1016/j.applthermaleng.2015.12.117

[23] Wang, Y., Numerical Study Of Hydrodynamics And Thermal Characteristics Of Heat Exchangers With Delta Winglets, *Thermal Science, 24* (2020), *1A*, pp. 325-338

[24] Naik, H., Tiwari, S., Thermodynamic Performance Analysis Of An Inline Fin-Tube Heat Exchanger In Presence Of Rectangular Winglet Pairs, *International Journal of Mechanical Sciences, 193* (2021), pp. 106148 https://doi.org/10.1016/j.ijmecsci.2020.106148

[25] ***, ANSYS, Fluent User's Guide, ANSYS, Inc., 2023

[26] Pauli, D., Estudo Experimental Da Troca De Calor Convectiva Em Matrizes Tubulares: Efeitos De Promotores De Turbulência Do Tipo Asa Delta (Experimental Study Of Convective Heat Exchange In Tubular Matrixes: Effects Of Turbulence Promoters Of Delta Type), B. Sc. Thesis, State University of Santa Catarina, Joinville, Brazil, 2014.

[27] Grimison, E. D., Correlation And Utilization Of New Data On Flow Resistance And Heat Transfer For Cross Flow Of Gases Over Tube Banks, *ASME. Trans., 59* (1937), 7, pp. 583–594

[28] Zhukauskas, A., Heat Transfer From Tubes in Cross Flow, *Advance in Heat Transfer, 8* (1972), pp. 93-160 https://doi.org/10.1016/S0065-2717(08)70038-8

Paper submitted: 10.10.2023.

Paper revised: 12.12.2023.

Paper accepted: 18.12.2023.